



CMB and Large-Scale Structure of the Universe

Nicola Vittorio 65-th birthday

Primordial non-Gaussianity

Sabino Matarrese

- Physics & Astronomy Dept. “G. Galilei”, University of Padova, Italy
- INFN Sezione di Padova
- INAF Osservatorio Astronomico di Padova
- GSSI L’Aquila



The present view on Primordial non-Gaussianity (PNG) in cosmological perturbations

- ✓ Alternative structure formation models of the late eighties considered strongly non-Gaussian primordial fluctuations.
- ✓ The increased accuracy in CMB and LSS observations has, however, excluded such an extreme possibility.
- ✓ The present-day challenge is to either detect or constrain **mild or weak** deviations from primordial Gaussian initial conditions.
- ✓ Deviations of this type are not only possible but are generically predicted in the standard perturbation generating mechanism provided by inflation.

“Standard” PNG model

Many primordial (inflationary) models of non-Gaussianity can be represented in configuration space by the simple formula (Salopek & Bond 1990; Gangui et al. 1994; Verde et al. 1999; Komatsu & Spergel 2001)

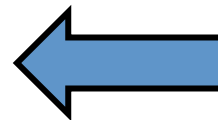
$$\Phi = \phi_L + f_{\text{NL}} * (\phi_L^2 - \langle \phi_L^2 \rangle) + g_{\text{NL}} * (\phi_L^3 - \langle \phi_L^2 \rangle \phi_L) + \dots$$

where Φ is the large-scale gravitational potential (more precisely $\Phi = 3/5 \zeta$ on superhorizon scales, where ζ is the gauge-invariant comoving curvature perturbation), ϕ_L its linear Gaussian contribution and f_{NL} the dimensionless non-linearity parameter (or more generally non-linearity function). The percent of non-Gaussianity in CMB data implied by this model is

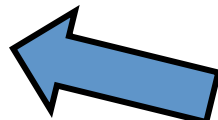
$$\text{NG \%} \sim 10^{-5} |f_{\text{NL}}|$$

$$\sim 10^{-10} |g_{\text{NL}}|$$

“non-Gaussian = non-dog”
(Ya.B. Zel’dovich)



< 10⁻⁵ from
CMB & LSS



< 10⁻⁵ from
CMB & LSS

PNG and bispectrum (shapes)

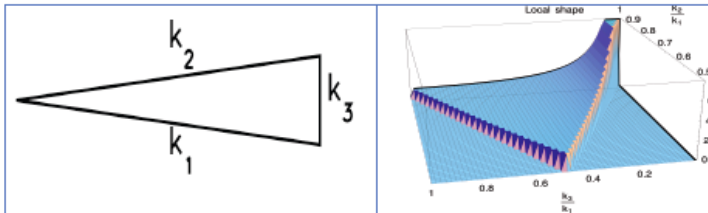
Bispectrum of primordial curvature perturbations

Amplitude

Shape

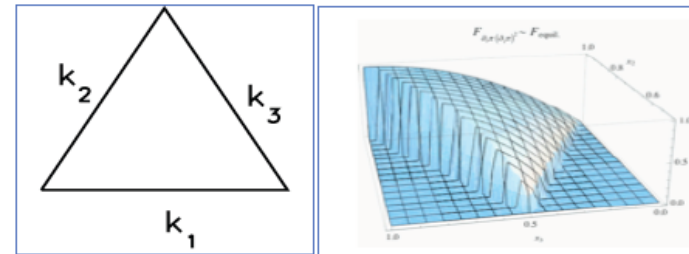
$$\langle \Phi(\vec{k}_1) \Phi(\vec{k}_2) \Phi(\vec{k}_3) \rangle = (2\pi)^3 \delta^{(3)}(\vec{k}_1 + \vec{k}_2 + \vec{k}_3) f_{\text{NL}} F(k_1, k_2, k_3)$$

Local NG



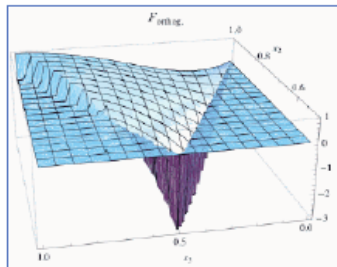
Multi-field models of inflation;
Cuvaton models;
Ekpyrotic/cyclic models

Equilateral NG



Single inflaton with non-standard kinetic term;
higher derivative interactions

Orthogonal NG



Single inflaton with non-standard kinetic term;
higher derivative interactions

Also: directionally dependent bispectra,
tensor bispectra and many others.

Bispectrum & PNG: theoretical expectations

- Primordial NG probed fundamental physics during inflation, being sensitive to **(self-)interactions** of fields present during inflation (different inflationary models predict different **amplitudes and shapes** of the bispectrum)
- Standard models of slow-roll inflation predict only a **tiny deviation from Gaussianity** (Salopek & Bond '90; Gangui, Lucchin, Matarrese & Mollerach 1995; Acquaviva, Bartolo, Matarrese & Riotto 2003; Maldacena 2003), arising from **non-linear gravitational interactions** during inflation.

Planck results are fully consistent with such a prediction!

- Searching for deviations from this *standard paradigm* is interesting *per-se*, for theoretically well-motivated models of inflation and, as shown in *Planck results*, can **severely limit** various classes of inflationary models beyond the simplest paradigm. PNG probes interactions among particles at inflation energy scales. See literature on probing string-theory via oscillatory PNG (Arkani-Hamed & Maldacena 2015 “Cosmological collider physics”; Silverstein 2017 “*The dangerous irrelevance of string theory*”).

PNG and precision cosmology

- PNG is currently the highest precision test of Standard Inflation models. With Planck:
 - PNG constrained at better than $\sim 0.01\%$
 - Flatness constrained at $\sim 0.1\%$
 - Isocurvature mode constrained at $\sim 1\%$.

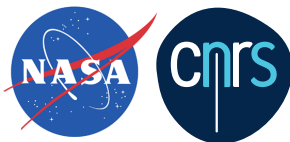
Warning: this is not a blind search for PNG

- Detecting non-zero primordial bispectrum (e.g. non-zero f_{NL}) proves that the initial seeds were non-Gaussian. Similarly for the trispectrum, etc. ...
- But: not detecting non-zero f_{NL} doesn't prove Gaussianity!
- There are infinitely many ways PNG can evade observational bounds optimized to search for f_{NL} and similar higher-order parameters

The scientific results that we present today are a product of the **Planck Collaboration**, including individuals from more than **100 scientific institutes** in Europe, the USA and Canada



planck



DTU Space
National Space Institute

Science & Technology
Facilities Council



National Research Council of Italy



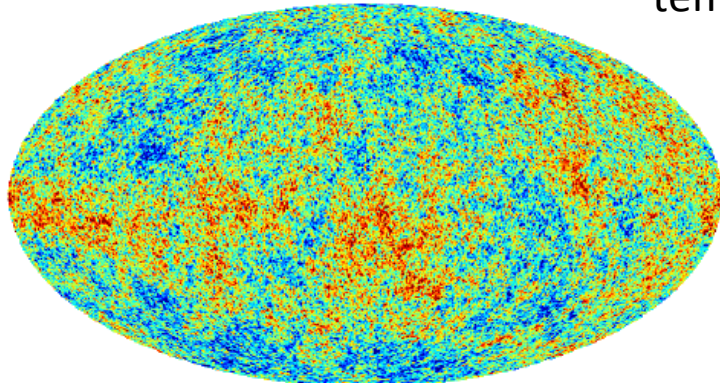
Planck is a project of the European Space Agency, with instruments provided by two scientific Consortia funded by ESA member states (in particular the lead countries: France and Italy) with contributions from NASA (USA), and telescope reflectors provided in a collaboration between ESA and a scientific Consortium led and funded by Denmark.

NG CMB simulated maps

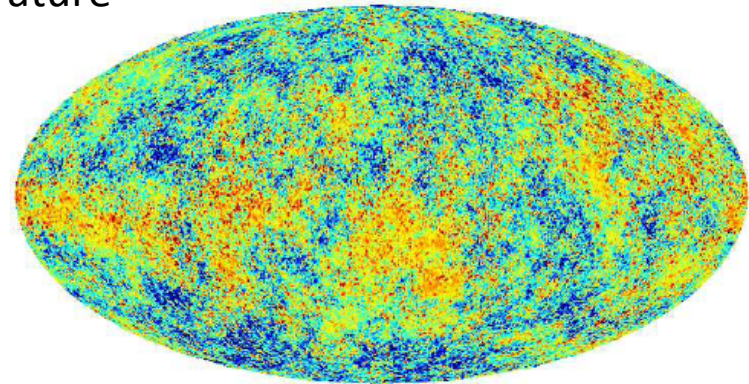
Temperatur $f_{NL}=0$

temperature

Temperature $f_{NL}=3000$



-0.25 0.25 mK



-0.25 0.25 mK

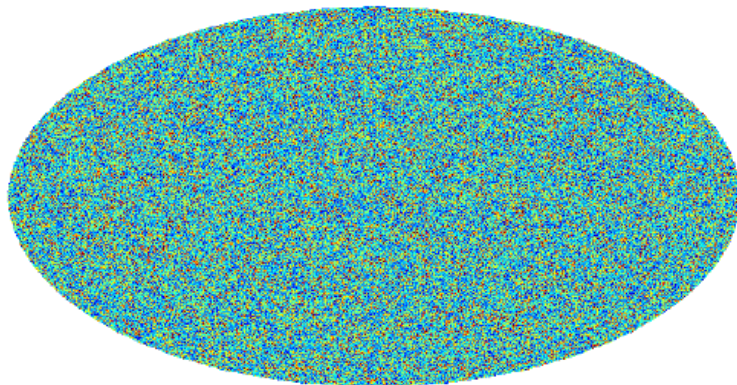
Gaussian

Liguori, Yadav, Hansen, Komatsu, Matarrese & Wandelt 2007

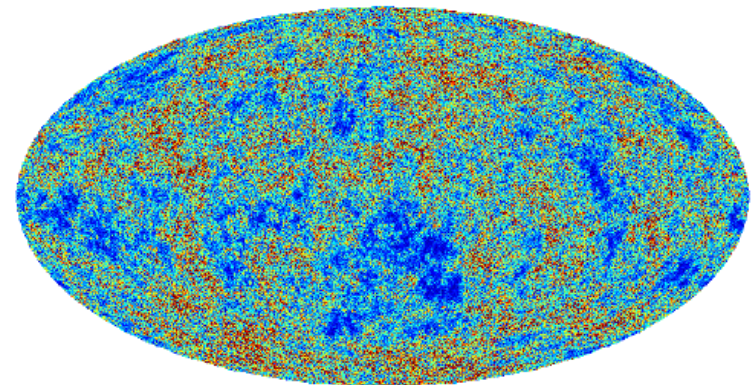
non-Gaussian

Polarization amplitude $f_{NL}=0$

Polarization amplitude $f_{NL}=3000$



0.0 0.0080 mK



0.0 0.0080 mK

polarization

Planck 2018 results IX: *Planck* collaboration, in preparation (2019)

PNG Planck project (Coordinators: S. Matarrese & B. Wandelt)

- Constrain (with high precision) and/or detect primordial non-Gaussianity (NG) as due to (non-standard) inflation (NG amplitude and shape measure deviations from standard inflation, perturbation generating processes after inflation, initial state before inflation, ...)
- We test: ***local, equilateral, orthogonal*** shapes (+ many more) for the bispectrum and constrain primordial trispectrum parameter g_{NL} (τ_{NL} constrained in previous release).
- We are completing (delivered in a few more weeks) a final, *Planck* legacy release, which will improve the 2015 results in terms of more refined treatment of E-mode polarization (including lower and higher l).

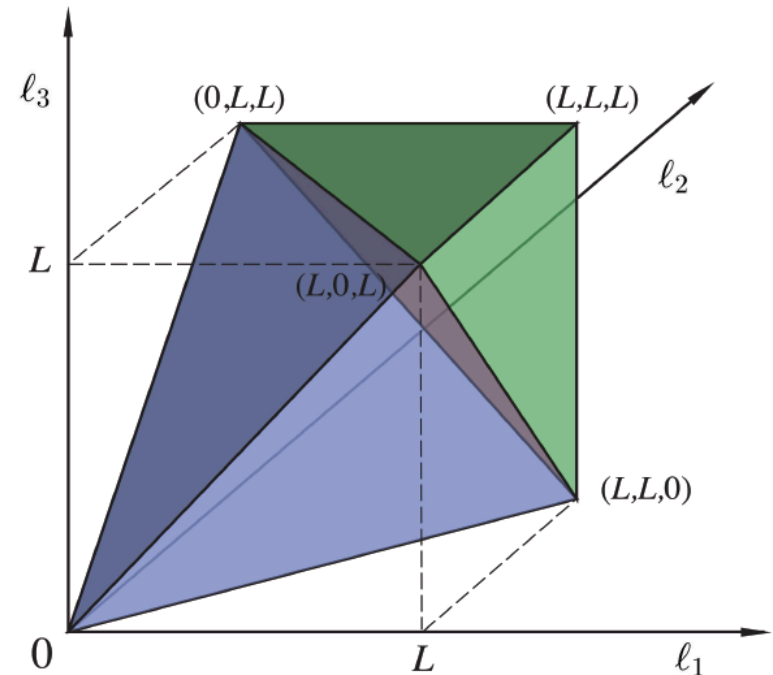
CMB bispectrum representation

$$B_{\ell_1 \ell_2 \ell_3}^{m_1 m_2 m_3} \equiv \langle a_{\ell_1 m_1} a_{\ell_2 m_2} a_{\ell_3 m_3} \rangle$$

$$= \mathcal{G}_{m_1 m_2 m_3}^{\ell_1 \ell_2 \ell_3} b_{\ell_1 \ell_2 \ell_3}$$

Gaunt integrals

$$\begin{aligned} \mathcal{G}_{m_1 m_2 m_3}^{\ell_1 \ell_2 \ell_3} &\equiv \int Y_{\ell_1 m_1}(\hat{\mathbf{n}}) Y_{\ell_2 m_2}(\hat{\mathbf{n}}) Y_{\ell_3 m_3}(\hat{\mathbf{n}}) d^2 \hat{\mathbf{n}} \\ &= h_{\ell_1 \ell_2 \ell_3} \begin{pmatrix} \ell_1 & \ell_2 & \ell_3 \\ m_1 & m_2 & m_3 \end{pmatrix}, \end{aligned}$$



Triangle condition: $\ell_1 \leq \ell_2 + \ell_3$ for $\ell_1 \geq \ell_2, \ell_3$, +perms.

Parity condition: $\ell_1 + \ell_2 + \ell_3 = 2n$, $n \in \mathbb{N}$,

Resolution: $\ell_1, \ell_2, \ell_3 \leq \ell_{\max}$, $\ell_1, \ell_2, \ell_3 \in \mathbb{N}$.

Optimal f_{NL} bispectrum estimator

$$\hat{f}_{NL} = \frac{1}{N} \sum B_{\ell_1 \ell_2 \ell_3}^{m_1 m_2 m_3} (C^{-1} a)_{\ell_1}^{m_1} (C^{-1} a)_{\ell_2}^{m_2} (C^{-1} a)_{\ell_3}^{m_3} - 3C_{\ell_1 m_1 \ell_2 m_2}^{-1} (C^{-1} a)_{\ell_3}^{m_3}$$

Leaving aside complications coming from breaking of statistical isotropy (sky-cut, noise, ...), one can see that we are extracting the 3-point function from the data and fitting theoretical bispectrum templates to it

$$\hat{f}_{NL} = \frac{1}{N} \sum_{\ell_i m_i} B_{\ell_1 \ell_2 \ell_3}^{m_1 m_2 m_3} \frac{a_{\ell_1}^{m_1}}{C_{\ell_1}} \frac{a_{\ell_2}^{m_2}}{C_{\ell_2}} \frac{a_{\ell_3}^{m_3}}{C_{\ell_3}}$$

A brute force implementation scales like ℓ_{\max}^5 . Unfeasible at Planck (or WMAP) resolution.

Can achieve massive speed improvement (ℓ_{\max}^3 scaling) if the reduced bispectrum is *separable* (KSW method: Komatsu, Spergel, Wandelt 2003).

$$b_{\ell_1 \ell_2 \ell_3} = \sum_{ijk} X_{\ell_1}^i Y_{\ell_2}^j Z_{\ell_3}^k \Rightarrow B_{\ell_1 \ell_2 \ell_3}^{m_1 m_2 m_3} = b_{\ell_1 \ell_2 \ell_3} \int Y_{\ell_1}^{m_1}(\Omega) Y_{\ell_2}^{m_2}(\Omega) Y_{\ell_3}^{m_3}(\Omega)$$

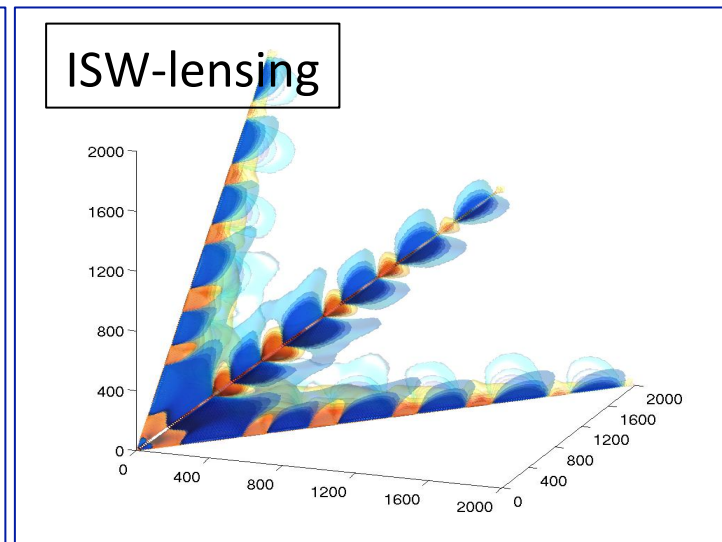
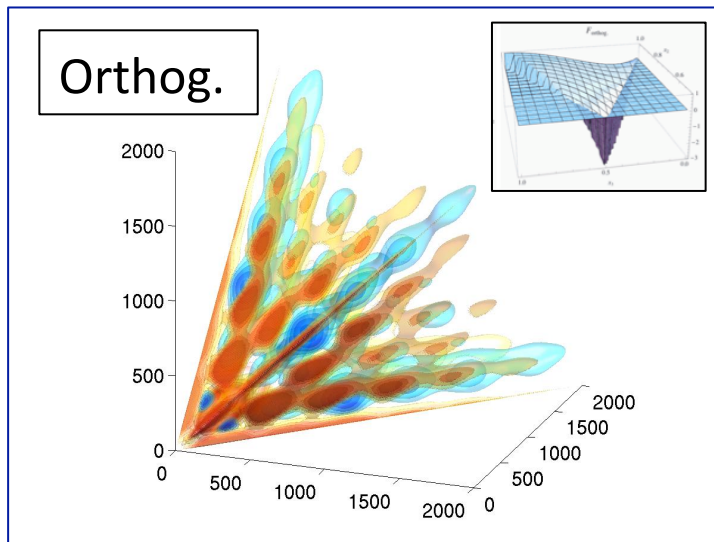
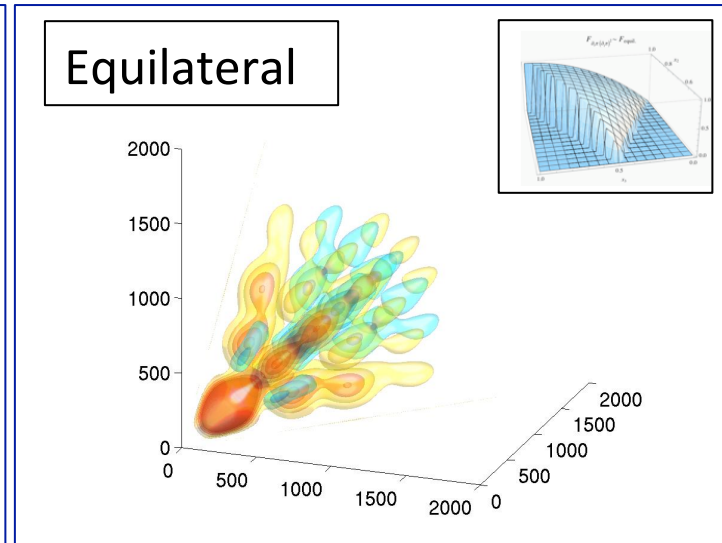
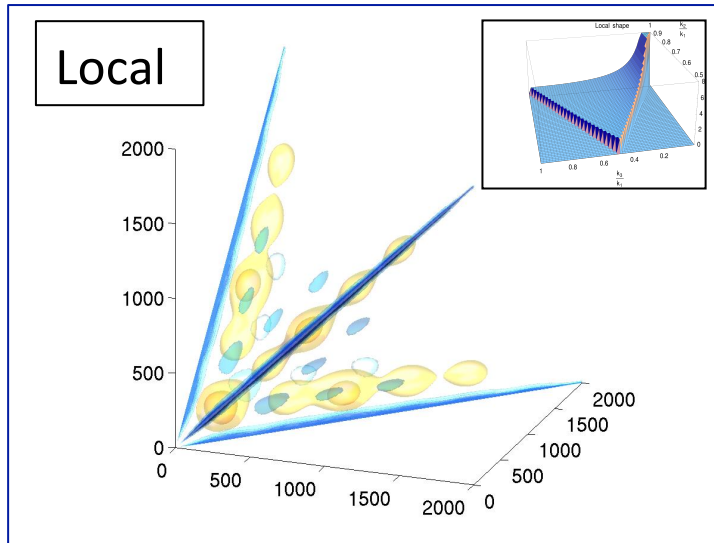
Optimal f_{NL} bispectrum estimator

$$\hat{f}_{NL} = \frac{1}{N} \sum B_{\ell_1 \ell_2 \ell_3}^{m_1 m_2 m_3} \left[(C^{-1}a)_{\ell_1}^{m_1} (C^{-1}a)_{\ell_2}^{m_2} (C^{-1}a)_{\ell_3}^{m_3} - 3C_{\ell_1 m_1 \ell_2 m_2}^{-1} (C^{-1}a)_{\ell_3}^{m_3} \right]$$

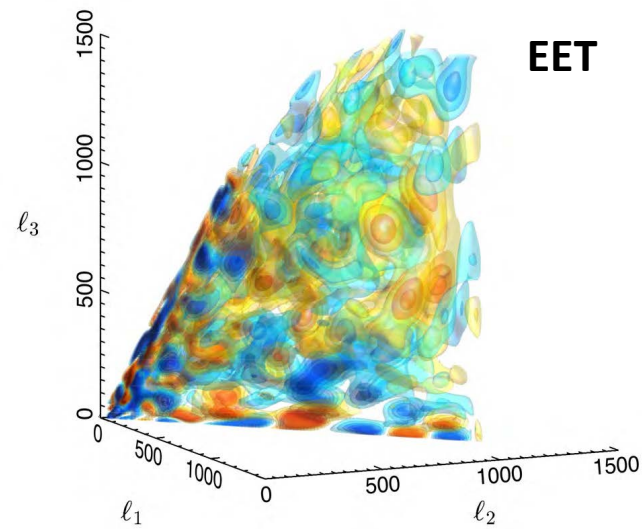
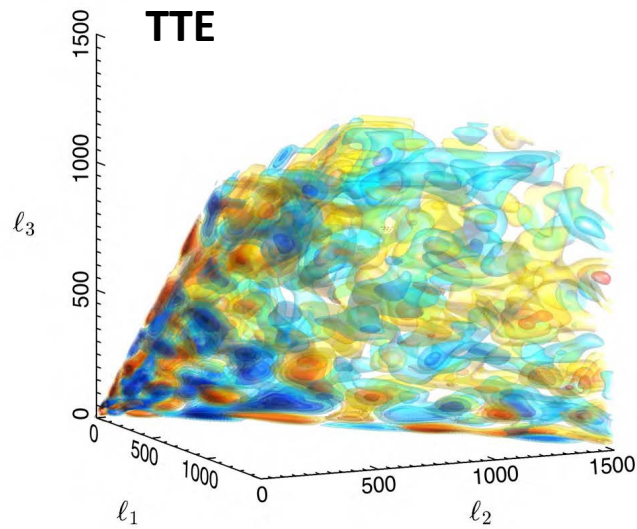
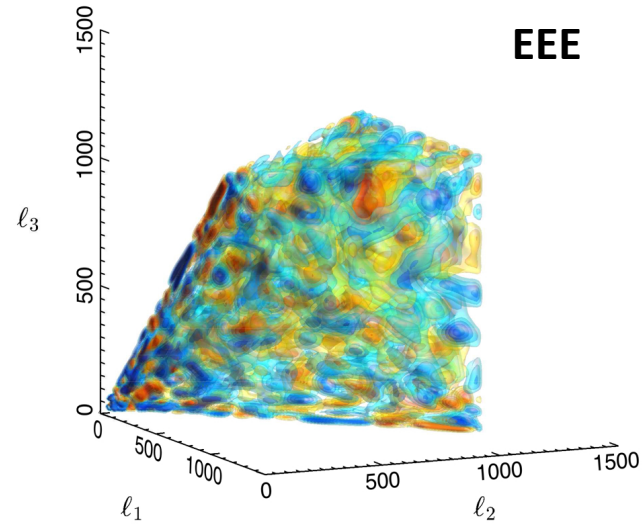
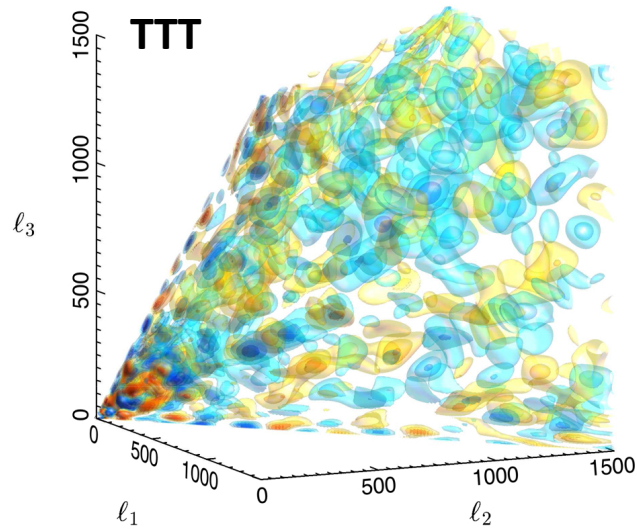
The theoretical template needs to be written in separable form. This can be done in different ways and *alternative implementations differ basically in terms of the separation technique adopted and of the projection domain.*

- KSW (Komatsu, Spergel & Wandelt 2003) separable template fitting + Skew-C_l extension (Munshi & Heavens 2010)
- Binned bispectrum (Bucher, Van Tent & Carvalho 2009)
- Modal expansion (Fergusson, Liguori & Shellard 2009)

Bispectrum shapes (modal representation)



The *Planck* bispectrum (modal; 2015)



(S/N weighted)

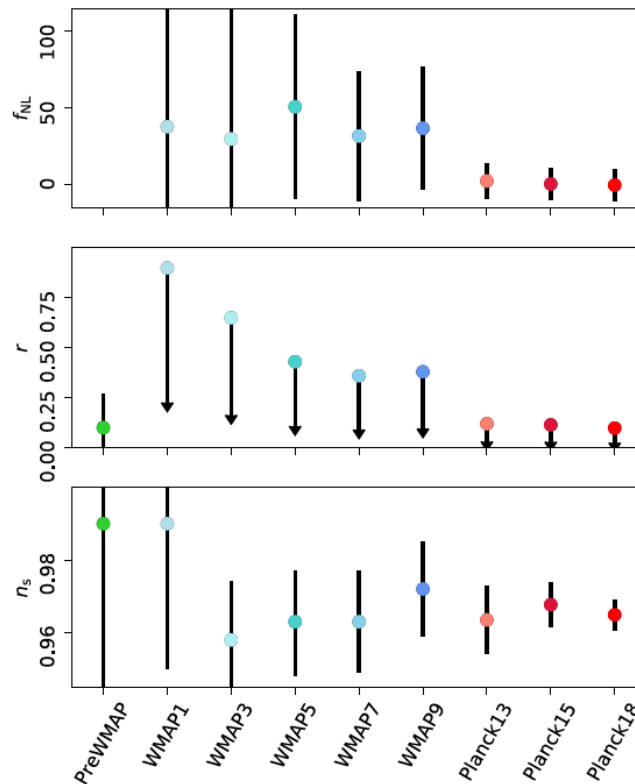
f_{NL} from *Planck* 2018 bispectrum (KSW)

Shape and method	$f_{\text{NL}}(\text{KSW})$		2015
	Independent	ISW-lensing subtracted	
SMICA (T)			
Local	5.9 ± 5.5	-1.6 ± 5.5	1.8 ± 5.6
Equilateral	13 ± 66	14 ± 66	-9.2 ± 69
Orthogonal	-37 ± 36	-15 ± 36	-20 ± 33
SMICA (T+E)			
Local	4.1 ± 5.1	-0.83 ± 5.1	0.71 ± 5.1
Equilateral	-17 ± 47	-18 ± 47	-9.5 ± 44
Orthogonal	-46 ± 23	-37 ± 23	-25 ± 22

$$l_{\text{min}} = 4$$

Preliminary

Evolution of CMB constraints on inflation parameters

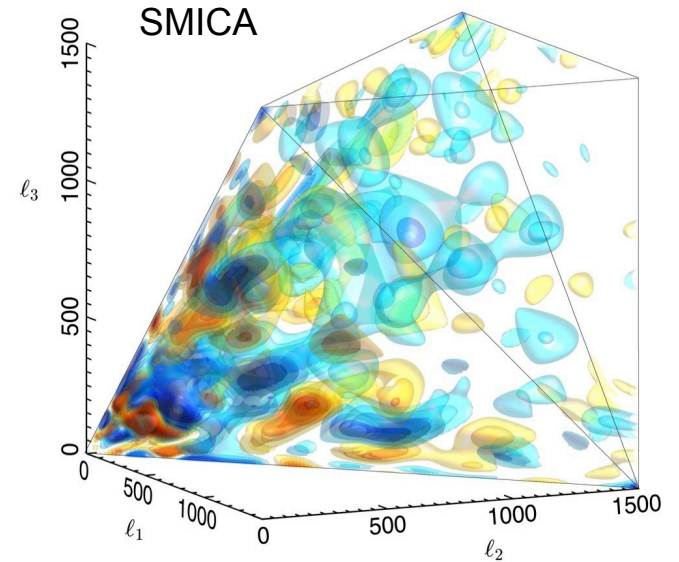


Planck collaboration
2018 (legacy paper)

Fig. 11. Evolution of CMB constraints on parameters describing “early Universe physics,” specifically the amount of primordial, local non-Gaussianity (f_{NL}), the tensor-to-scalar ratio (r), and the slope of the primordial power spectrum (n_s).

ISW-lensing bispectrum from *Planck*

The coupling between weak lensing and Integrated Sachs-Wolfe (ISW) effects is the leading contamination to local NG. We have detected the ISW-lensing bispectrum with a significance of $\sim 3\sigma$. This determination is also robust to SZ removal (2019).



SMICA (T+E)

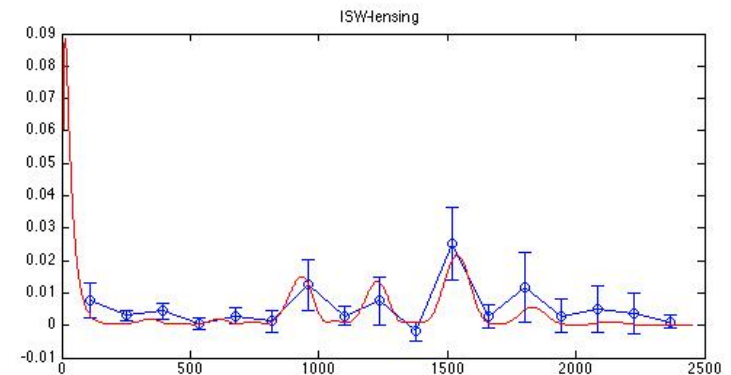
$$f_{NL}^{ISW-lensing} = 0.81 \pm 0.27$$

SMICA-noSZ (T+E)

$$f_{NL}^{ISW-lensing} = 0.90 \pm 0.28$$

Preliminary

Skew- C_l detection of ISW-lensing signal



Planck constraints on primordial trispectrum amplitudes

- In the 2018 release we obtain also constraints on 3 fundamental shapes of the trispectrum (transform of 4-pt function)

Trispectrum	Value
g_{nl}^{loc}	$(-5.3 \pm 9.3) \times 10^4$
$g_{nl}^{\dot{\pi}^4}$	$(-2.1 \pm 2.0) \times 10^6$
$g_{nl}^{(\partial\pi)^4}$	$(-6.0 \pm 5.0) \times 10^6$

Preliminary

Standard inflation still alive ... and kicking!

Standard inflation

- single scalar field (*single clock*)
- canonical kinetic term
- slow-roll dynamics
- Bunch-Davies initial vacuum state
- Einstein gravity

predicts tiny (up to $O(10^{-2})$, or even less??) primordial NG signal

→ No presently detectable PNG

Beyond “standard” shapes

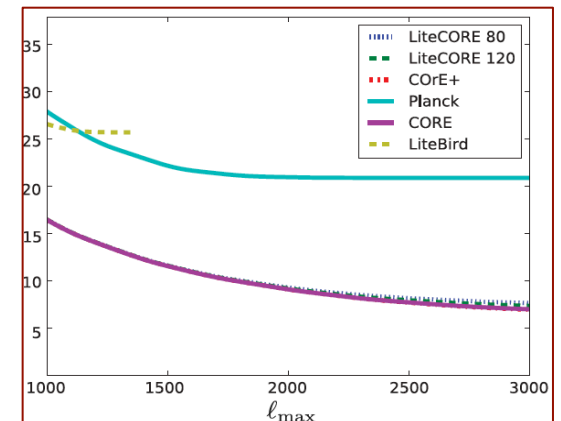
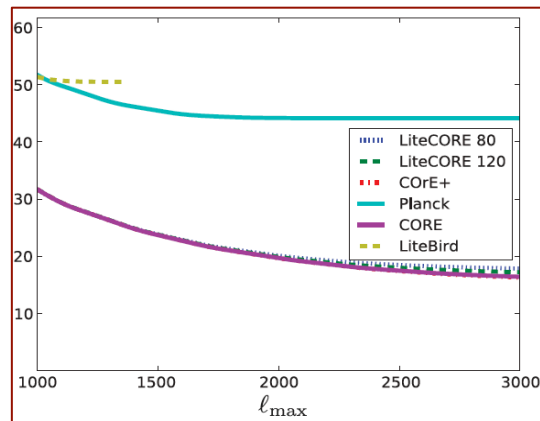
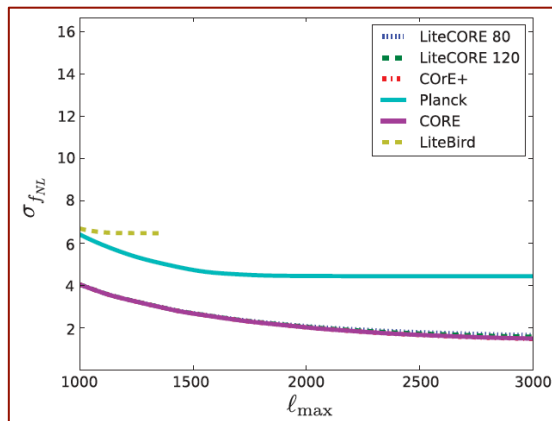
We constrain f_{NL} for a large number of primordial models beyond the standard local, equilateral, orthogonal shapes, including

- ✓ Equilateral family (DBI, EFT, ghost)
 - ✓ Flattened shapes (non-Bunch Davies)
 - ✓ Feature models (oscillatory bispectra, scale-dependent)
 - ✓ Direction dependence
 - ✓ Quasi-single-field
 - ✓ Parity-odd models
- No evidence for PNG found → constraints on parameters from the models above

CORE: CMB bispectrum forecasts

	LiteCORE 80	LiteCORE 120	CORE M5	COrE+	Planck 2015	LiteBIRD	ideal 3000
T local	4.5	3.7	3.6	3.4	(5.7)	9.4	2.7
T equilat	65	59	58	56	(70)	92	46
T orthog	31	27	26	25	(33)	58	20
T lens-isw	0.15	0.11	0.10	0.09	(0.28)	0.44	0.07
E local	5.4	4.5	4.2	3.9	(32)	11	2.4
E equilat	51	46	45	43	(141)	76	31
E orthog	24	21	20	19	(72)	42	13
E lens-isw	0.37	0.29	0.27	0.24		1.1	0.14
T+E local	2.7	2.2	2.1	1.9	(5.0)	5.6	1.4
T+E equilat	25	22	21	20	(43)	40	15
T+E orthog	12	10.0	9.6	9.1	(21)	23	6.7
T+E lens-isw	0.062	0.048	0.045	0.041		0.18	0.027

from: Finelli et al. 2018



PNG vs. Large-Scale Structure (LSS)

PNG in LSS (to make contact with the CMB definition) can be defined through a potential Φ defined starting from the DM density fluctuation δ through Poisson's equation (use comoving gauge for density fluctuation, Bardeen 1980)

$$\delta = -\left(\frac{3}{2}\Omega_m H^2\right)^{-1} \nabla^2 \Phi$$

Assuming the same model

$$\Phi = \phi_L + f_{NL} (\phi_L^2 - \langle \phi_L^2 \rangle) + g_{NL} (\phi_L^3 - \langle \phi_L^2 \rangle \phi_L) + \dots$$

Φ on sub-horizon scales reduces to minus the large-scale gravitational potential, ϕ_L is the linear Gaussian contribution and f_{NL} and g_{NL} are dimensionless non-linearity parameters (or more generally non-linearity functions).

CMB and LSS conventions may differ by a factor 1.3 for f_{NL} , $(1.3)^2$ for g_{NL}

N-body simulations with NG initial data

$$\Phi = \Phi_L + f_{NL}(\Phi_L^2 - \langle \Phi_L^2 \rangle)$$

$$\nabla^2(\Phi * T)g(z) = -4\pi G a^2 \delta\rho_{DM}$$

growth suppression factor

matter transfer function

Grossi, Moscardini, Dolag, Branchini, Matarrese & Moscardini (2007)

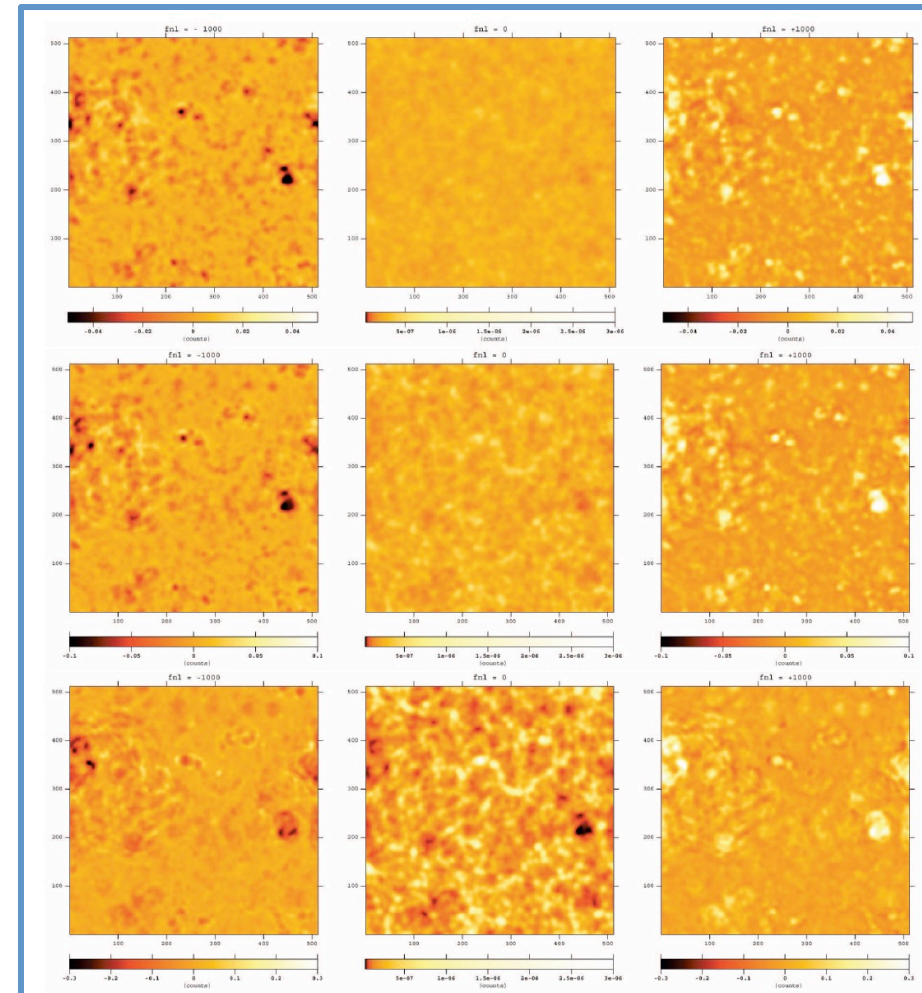


Figure 1. Slice maps of simulated mass density fields at $z = 5.15$ (top), $z = 2.13$ (middle) and $z = 0$ (bottom). The number of pixels at a side length is 512 ($300h^{-1}\text{Mpc}$) and that of the thickness is 32 ($31.25h^{-1}\text{Mpc}$). The panels in the middle row show the log of the projected density smoothed with a Gaussian filter of 10 pixels width, corresponding to $9.8h^{-1}\text{Mpc}$. The left and right panels are the relative residuals for the $f_{NL} = \pm 1000$ runs (equation [17]). Each panel has the corresponding color bar and the range considered are different from panel to panel.

Searching for PNG with rare events

- Besides using standard statistical estimators, like (mass) bispectrum, trispectrum, three and four-point function, skewness, etc. ..., one can look at the tails of the distribution, i.e. at rare events.
- Rare events have the advantage that they often maximize deviations from what is predicted by a Gaussian distribution, but have the obvious disadvantage of being rare! But remember that, according to Press-Schechter-like schemes, all collapsed DM halos correspond to (rare) high peaks of the underlying density field (note: density, not gravitational potential maxima).
- Analogous to hot and cold spots in CMB maps (Matarrese & Vittorio (2019, in preparation), extending previous work on Gaussian fields (Vittorio & Juszkiewicz 1987).
- Matarrese, Verde & Jimenez (2000) and Verde, Jimenez, Kamionkowski & Matarrese showed that clusters at high redshift ($z > 1$) can probe NG down to $f_{\text{NL}} \sim 10^2$. Many more analyses and predictions afterwards. Excellent agreement of analytical formulae with N-body simulations found by Grossi et al. 2009; Desjacques et al. 2009; Pillepich et al. 2010; ... and many others.
- Halo (galaxy) clustering 2-point and higher-order correlation functions represent further and more powerful implementations of this general idea (Dalal et al. 2007; Matarrese & Verde 2008; Giannantonio & Porciani 2010; Baldauf et al. 2011).

Dark matter halo clustering as a powerful constraint on PNG

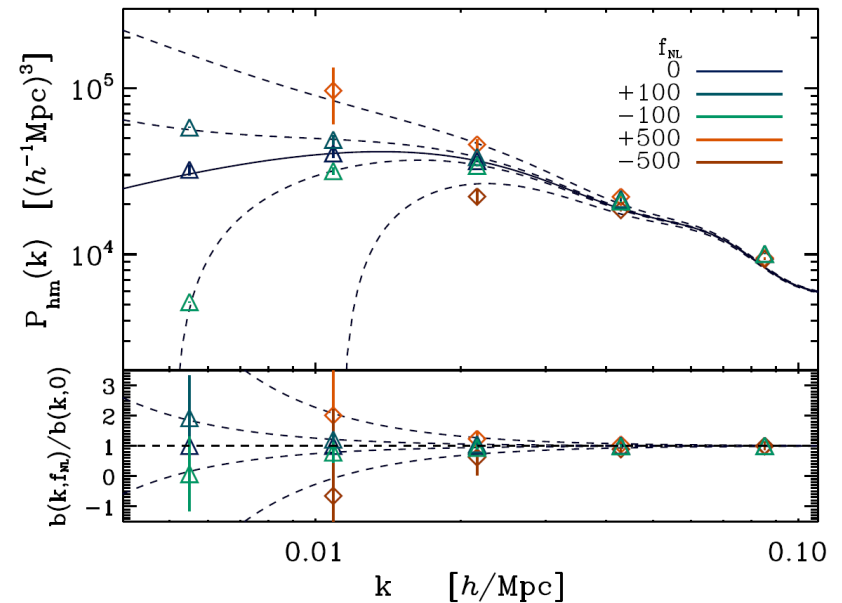
$$\delta_{\text{halo}} = b \delta_{\text{matter}}$$

Dalal et al. (2007) have shown that halo bias is sensitive to primordial non-Gaussianity through a scale-dependent correction term (in Fourier space)

$$\Delta b(k)/b \propto 2 f_{\text{NL}} \delta_{\text{c}} / k^2$$

This opens interesting prospects for constraining or measuring NG in LSS but demands for an accurate evaluation of the effects of (general) NG on halo biasing.

Dalal, Dore', Huterer & Shirokov 2007



Clustering of peaks (DM halos) of NG density field

Start from results obtained in the 80's by Grinstein & Wise 1986, Matarrese, Lucchin & Bonometto 1986, Lucchin, Matarrese & Vittorio 1988) giving the general expression for the peak 2-point function as a function of N-point connected correlation functions of the background linear (i.e. **Lagrangian**) mass-density field

$$\xi_{h,M}(|\mathbf{x}_1 - \mathbf{x}_2|) = -1 + \exp \left\{ \sum_{N=2}^{\infty} \sum_{j=1}^{N-1} \frac{\nu^N \sigma_R^{-N}}{j!(N-j)!} \xi^{(N)} \left[\begin{matrix} \mathbf{x}_1, \dots, \mathbf{x}_1, & \mathbf{x}_2, \dots, \mathbf{x}_2 \\ j \text{ times} & (N-j) \text{ times} \end{matrix} \right] \right\}$$

(requires use of path-integral, cluster expansion, multinomial theorem and asymptotic expansion). The analysis of NG models was motivated by a paper by Vittorio, Juszkiewicz and Davis (1986) on bulk flows.

THE ASTROPHYSICAL JOURNAL, 330:L21-L23, 1988 July 1
© 1988. The American Astronomical Society. All rights reserved. Printed in U.S.A.

SCALE-INVARIANT CLUSTERING AND PRIMORDIAL BIASING

FRANCESCO LUCCHIN AND SABINO MATARRESE
Dipartimento di Fisica, G. Galilei, Università di Padova

AND

NICOLA VITTORIO
Dipartimento di Fisica, Università dell'Aquila
Received 1987 December 14; accepted 1988 March 31

ABSTRACT

If cosmic objects formed around the maxima of a scale-invariant (either Gaussian or non-Gaussian) density perturbation field, their correlation length and mean distance are proportional as suggested by the observations. Since the typical density contrast of a peak is ν times greater than the field rms value, a size-independent, primordial threshold ν is obtained whose magnitude depends only on the statistics; late nonlinear evolution would mainly affect the clustering properties of objects like galaxies. In this framework we discuss a simple, phenomenological model for the power-spectrum and a "minimal," isocurvature perturbation model.

Subject headings: cosmology — galaxies: clustering — galaxies: formation

Recent analyses of the clustering properties of galaxies, groups, and clusters suggest that their coherence length is a growing function of the richness (Davis and Peebles 1983; Bahcall and Soneira 1983; Klypin and Kopylov 1983; Schectman 1985). All the observed two-point correlation functions are well described by a single power law, $\xi(r) \approx (r/r_0)^{-1.8}$ in a suitable range of distances. The coherence lengths $r_c \approx 5h^{-1}$ Mpc (h is the Hubble constant in units of $100 \text{ km s}^{-1} \text{ Mpc}^{-1}$) and $r_c \approx 25h^{-1}$ Mpc refer to galaxies and clusters, respectively. A similar trend seems to hold for superclusters, with $r_c \approx 50h^{-1}$ Mpc (Bahcall and Burgett 1986). Szalay and Schramm (1982) have shown that the systematic change of r_c with the system richness approximately vanishes if r_c is made dimensionless using the mean interparticle distance l_c . They find $r_c/l_c \approx 0.56$, with the only exception of galaxies, which appear to have $r_c/l_c \approx 1$. Recent analyses (see, e.g., Sutherland 1988) seem to provide a smaller value for r_c and suggest that previous results would deserve some caution.

If the trend for r_c is confirmed it follows that different objects cannot be at once tracers of the overall density field. On the other hand, rich systems are rare and one can reconcile theory and observations by properly doing the statistics of rare events. This approach has been used to explain the different coherence lengths of galaxies and rich Abell clusters (Kaiser 1984; Politzer and Wise 1984; Bardeen *et al.* 1986; Martínez-González and Sanz 1988). It is plausible that the formation of objects is biased to occur around the maxima of the density field (i.e., the minima of the potential fluctuations). Peacock and Heavens (1985) found that the typical maxima of a Gaussian random field have a density contrast $\nu \approx 2$ times greater than the field rms value, independently of the proto-object size. This property can be easily generalized to non-Gaussian, scale-invariant distributions, although the numerical value of ν can be different. For a Gaussian random field the correlation of the up-crossing regions is well approximated by the Politzer and Wise (1984) formula, $\xi_{\nu, \lambda}(r; R_i) \approx \exp[\nu^2 \xi(r; R_i)/\sigma^2(R_i)] - 1$, for $\nu_i \gg 1$. Here $\xi(r; R_i) = (2\pi^2)^{-1} \int_0^\infty dk k^2 P(k) \exp(-k^2 R_i^2) \sin kr / kr$ is the correlation of the overall density field, smoothed on the typical proto-object size R_i , $\sigma^2(R_i)$ is the mass

variance, and $P(k)$ is the power spectrum. By tuning R_i and ν_i it is possible to reproduce the observed coherence length of the distribution of objects of the i th richness class.

The purpose of this Letter is to show that a unique threshold ν for all the levels of the hierarchy would account for the scale-invariant (fractal) properties of the large-scale matter distribution suggested by observational data. As far as galaxies are concerned we attempt to recover their peculiar clustering properties by taking into account nonlinear gravitational effects on an initial Gaussian distribution. We discuss a simple, phenomenological model where $P(k) \propto k^{-1}$ and a "minimal," isocurvature perturbation model recently proposed by Peebles (1987).

Both the power-law behavior of all the observed correlation functions and the proportionality between the coherence length and the interparticle distance are commonly taken as an evidence for the scale-invariance of the underlying density fluctuation field. Under this assumption, the N -point (reduced) correlation functions obey to a simple scaling relation (Otto *et al.* 1986; Lucchin and Matarrese 1988):

$$\xi^{(N)}(\lambda \mathbf{x}_1, \dots, \lambda \mathbf{x}_N; \lambda R_i) = \lambda^{-N(3+n)/2} \xi^{(N)}(\mathbf{x}_1, \dots, \mathbf{x}_N; R_i), \quad (1)$$

n being the primordial spectral index. In this notation $\xi^{(2)}(0, 0; R)$ is the mass variance, which then scales according to $\sigma^2(\lambda R) = \lambda^{-(3+n)/2} \sigma^2(R)$. Independently of the assumed statistics, the correlation function of the up-crossing regions can be expressed as (Matarrese, Lucchin, and Bonometto 1986; Grinstein and Wise 1986)

$$1 + \xi_{\nu, \lambda}(|\mathbf{x}_1 - \mathbf{x}_2|; R_i) \approx \exp \left\{ \sum_{N=2}^{\infty} \sum_{j=1}^{N-1} \frac{\nu_i^N}{j!(N-j)!} \xi^{(N)} \left[\begin{matrix} \mathbf{x}_1, \dots, \mathbf{x}_1, & \mathbf{x}_2, \dots, \mathbf{x}_2 \\ j \text{ times} & (N-j) \text{ times} \end{matrix} ; R_i \right] \sigma^{-N}(R_i) \right\}. \quad (2)$$

This is the non-Gaussian generalization of the Politzer-Wise formula. If ν is kept fixed, equation (1) and equation (2) imply

Halo bias in NG models

Matarrese & Verde 2008

$$b_h^{f_{\text{NL}}} = 1 + \frac{\Delta_c(z)}{\sigma_R^2 D^2(z)} \left[1 + 2f_{\text{NL}} \frac{\Delta_c(z)}{D(z)} \frac{\mathcal{F}_R(k)}{\mathcal{M}_R(k)} \right]$$

form factor:

$$\mathcal{F}_R(k) = \frac{1}{8\pi^2 \sigma_R^2} \int dk_1 k_1^2 \mathcal{M}_R(k_1) P_\phi(k_1) \times \int_{-1}^1 d\mu \mathcal{M}_R(\sqrt{\alpha}) \left[\frac{P_\phi(\sqrt{\alpha})}{P_\phi(k)} + 2 \right]$$

$$\alpha = k_1^2 + k^2 + 2k_1 k \mu$$

factor connecting the smoothed linear overdensity with the primordial potential:

$$\mathcal{M}_R(k) = \frac{2}{3} \frac{T(k) k^2}{H_0^2 \Omega_{m,0}} W_R(k)$$

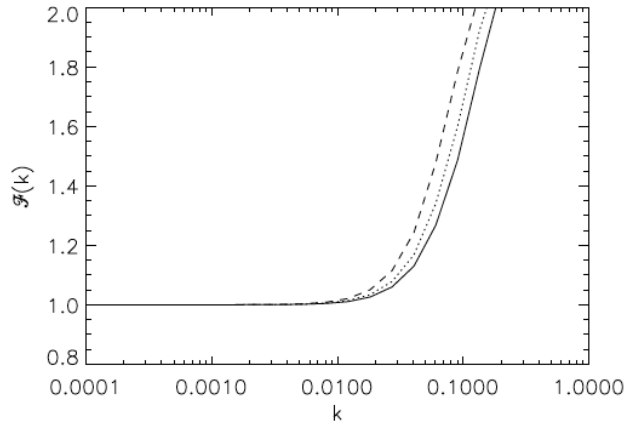


FIG. 1.— The function $\mathcal{F}_R(k)$ for three different masses: $1 \times 10^{14} M_\odot$ (solid), $2 \times 10^{14} M_\odot$ (dotted), $1 \times 10^{15} M_\odot$ (dashed).

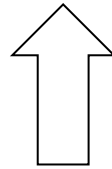
power-spectrum of a Gaussian gravitational potential

transfer function:

window function defining the radius R of a proto-halo of mass $M(R)$:

PNG with LSS: Bispectrum

Sample	Power Spectrum		Bispectrum	
	$\sigma_{f_{\text{NL}}}$ bias float	$\sigma_{f_{\text{NL}}}$ bias fixed	$\sigma_{f_{\text{NL}}}$ bias float	$\sigma_{f_{\text{NL}}}$ bias fixed
BOSS	21.30	13.28	1.04 ^(0.65) _(2.47)	0.57 ^(0.35) _(1.48)
eBOSS	14.21	11.12	1.18 ^(0.82) _(2.02)	0.70 ^(0.48) _(1.29)
Euclid	6.00	4.71	0.45 ^(0.18) _(0.71)	0.32 ^(0.12) _(0.35)
DESI	5.43	4.37	0.31 ^(0.17) _(0.48)	0.21 ^(0.12) _(0.37)
BOSS + Euclid	5.64	4.44	0.39 ^(0.17) _(0.59)	0.28 ^(0.11) _(0.34)



Tellarini et al. 2016

- Fisher matrix forecast. Tree-level bispectrum. Local NG initial conditions. In redshift space. Covariance between different triangles neglected (optimistic).
- The bispectrum could do better than the power-spectrum.
- $f_{\text{NL}} \sim 1$ achievable with forthcoming surveys?
- Many issues, e.g. full covariance, accurate bias model, GR effects, survey geometry, estimator implementation ... Still, great potential: 3D vs 2D (CMB).

GR approach to power-spectrum and bispectrum

- In full generality GR effects (including also redshift-space distortions, lensing, etc ...) have to be taken into account both in the galaxy power-spectrum and bispectrum, as well as in the DM evolution.
- Bertacca, Raccanelli, Bartolo, Liguori, Matarrese & Verde (2017) wrote down for the first time the complete expression for the galaxy bispectrum (whose expression is obviously VERY complex) to be soon compared with observations.

LSS initial conditions reconstruction to constrain/detect PNG

- PNG in LSS is contaminated by NG arising from non-linear gravitational evolution.
- Hence one can hope to improve PNG S/N by tracing LSS back in time and measure e.g. the bispectrum in reconstructed maps.
- Various reconstruction techniques have been proposed and tested, since the earliest proposal by Peebles (1989). For an application to PNG, see also Mohayaee, Mathis, Colombi & Silk 2006; based on MAK (Frisch, Matarrese, Mohayaee & Sobolevski 2002).
- Based upon recent results (Sarpa et al. 2018) aimed at reconstructing BAOs, Sarpa, Branchini, Carbone, Matarrese & Schimd are going to apply extended FAM algorithm (Nusser & Branchini 2000) with that purpose to N-body sims with non-Gaussian initial data.

BAO reconstruction: a swift numerical action method for massive spectroscopic surveys

[arXiv:1809.10738](https://arxiv.org/abs/1809.10738) [astro-ph.CO]

submitted to MNRAS

E. Sarpa,^{1,2*} C. Schmid,¹ E. Branchini,^{3,4,5} S. Matarrese.^{2,6,7,8}

¹ Aix Marseille Univ, CNRS, LAM, Laboratoire d'Astrophysique de Marseille, Marseille, France

² Dipartimento di Fisica e Astronomia "Galileo Galilei", Università degli studi di Padova, Via F. Marzolo, 8, I-35131 Padova, Italy

³ Dipartimento di Matematica e Fisica, Università degli studi Roma Tre, Via della Vasca Navale, 84, 00146 Roma, Italy

⁴ INFN - Sezione di Roma Tre, via della Vasca Navale 84, I-00146 Roma, Italy

⁵ INAF - Osservatorio Astronomico di Roma, via Frascati 33, I-00040 Monte Porzio Catone (RM), Italy

⁶ INFN, Sezione di Padova, via F. Marzolo 8, I-35131, Padova, Italy

⁷ INAF-Osservatorio Astronomico di Padova, Vicolo dell'Osservatorio 5, I-35122 Padova, Italy

⁸ Gran Sasso Science Institute, Viale F. Crispi 7, I-67100 L'Aquila, Italy

Idea: Reconstruction of the *full* trajectories of biased tracers (haloes, galaxies, ...) by minimisation of the action (Peebles 1989):

- orbits of i-th (point-like) object parametrised as $\mathbf{x}_i(D) = \mathbf{x}_{i,\text{obs}} + \sum_{n=0}^M \mathbf{C}_{i,n} q_n(D)$, with $\mathbf{C}_{i,n}$ unknown: $\mathbf{C}_{i,n} = \text{argmin } S$

$$\frac{S}{mH_0} = \sum_{i=0}^N \int_0^{D_{\text{obs}}} dD fED a^2 \frac{1}{2} \left(\frac{d\mathbf{x}_i}{dD} \right)^2 + \sum_{i=0}^N \int_0^1 dD \frac{3\Omega_{m0}}{8\pi fED} \frac{1}{a} \left[\frac{1}{n_{\text{obs}} a^3} \frac{1}{2} \sum_{j=0, j \neq i}^N \frac{1}{|\mathbf{x}_i - \mathbf{x}_j|} + \frac{2}{3} \pi \mathbf{x}_i^2 \right]$$

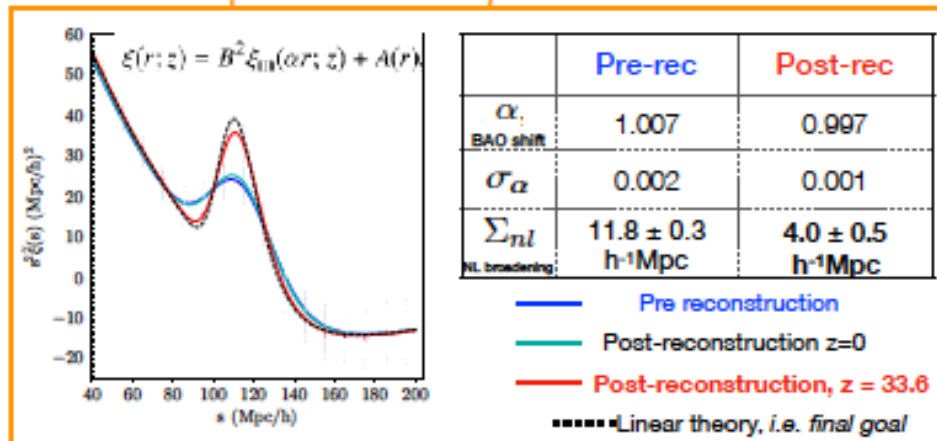
- mixed boundary conditions: observed positions + asymptotically vanishing initial velocities (i.e. initial homogeneity)
- FLRW universe (with generic, smooth dark-energy) + Newtonian approximation; equal mass particles; no merging

Target :	* Peebles ('90s):	Local group	~ 5 Mpc,	~ 10 ⁸ particles
	* Nusser & Branchini 2000 (FAM):	Local supercluster	~ 60 Mpc,	< 10 ⁴ particles
	* Sarpa et al. 2018 (eFAM):	Large Scale Structure	~ 2 Gpc,	10 ⁸ particles

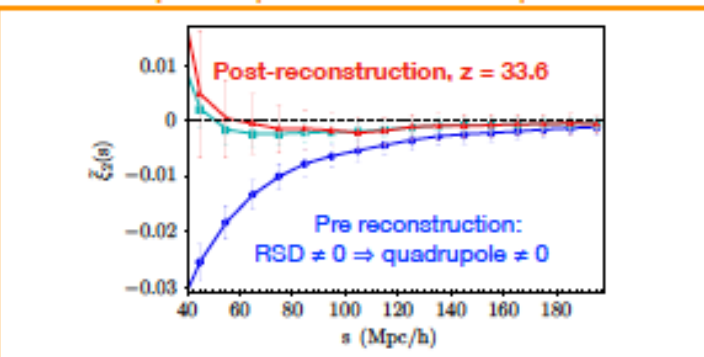
tested on dark-matter haloes from DEUS-FUR simulation

BAO reconstruction: a swift numerical action method for massive spectroscopic surveys

2-PCF: monopole in redshift space

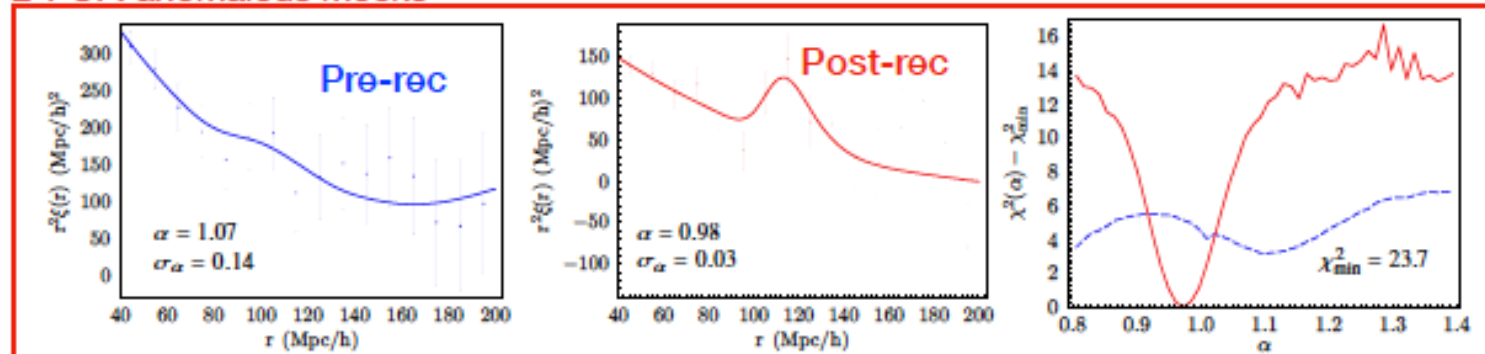


2-PCF: quadrupole in redshift space



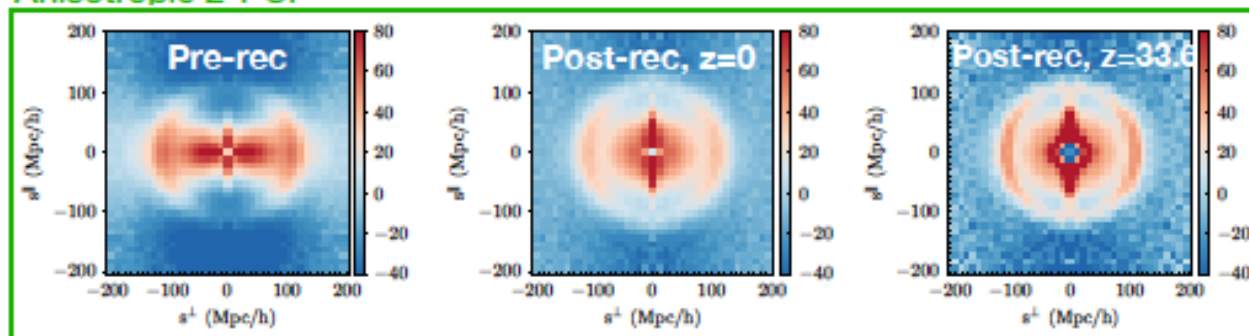
The new algorithm successfully reconstructs the BAO peak of linear theory, fully correcting for RSD on scale $> 50 h^{-1}\text{Mpc}$

2-PCF: anomalous mocks



The new algorithm successfully recovers the BAO peak in statistically anomalous samples with unclear BAO peak (low S/N)

Anisotropic 2-PCF



The new algorithm recovers the BAO ring at very-high S/N up to very large z (unlike standard method based on Zel'dovich approx, which after smoothing is limited to $z \sim 3$)

Controversial issue: is the single-field consistency relation observable?

The bispectrum for single-field inflation (Gangui et al. 1995; Acquaviva et al. 2001; Maldacena 2001) can be represented as:

$$B_{\zeta}(k_1, k_2, k_3) \propto \frac{(\Delta_{\zeta}^2)^2}{(k_1 k_2 k_3)^2} \left[(1 - n_s) \mathcal{S}_{\text{loc.}}(k_1, k_2, k_3) + \frac{5}{3} \varepsilon \mathcal{S}_{\text{equil.}}(k_1, k_2, k_3) \right]$$
$$n_s - 1 = -\eta - 2\varepsilon, \text{ with } \varepsilon \equiv -\frac{H}{H^2}, \eta \equiv \frac{\dot{\varepsilon}}{H\varepsilon}$$

The observability of the so-called “**Maldacena consistency relation**”, related to the above bispectrum for single field inflation, in CMB and LSS data has led to a long-standing controversy. Recently, various groups have argued that the $(1-n_s)$ term is totally unobservable (for single-clock inflation), as, in the strictly squeezed limit (one of the wave-numbers going to 0), this term can be gauged away by a local coordinate transformation. Cabass et al. (2017): this term survives up to a “renormalization” reduces it by a factor ~ 0.1 .

Matarrese, Pilo & Rollo (2018) reanalyzed the quantities generally used to perform PNG calculations, finding several inconsistencies. \rightarrow use only covariant and gauge-invariant definitions to get rid of ambiguities in the squeezed limit (Matarrese, Pilo & Rollo, in preparation): this will provide an **exact** description, not affected by “spurious PNG”. That is crucial to set lower bound on PNG for all inflation models.

Concluding remarks

- ✓ Inflation provides a causal mechanism for the generation of cosmological perturbations
- ✓ CMB and LSS data fully support the detailed predictions of inflation
- ✓ The direct detection of:
 - ☞ primordial **gravitational waves**
 - ☞ primordial **non-Gaussianity**

with the specific features predicted by inflation would provide strong independent support to the model.

The next challenge

- The next challenge is to measure $f_{\text{NL}} \sim 10^{-2}$

“The Challenge” (September 1993):



- Drive Nicola's car for the first time in Naples' traffic, from Naples (Molo Beverello) to Sant'Agata dei due Golfi.
- And ...I succeeded!
- Detecting $f_{NL} \sim 0.01$ is nothing compared to that!!